

A Traffic Signal Optimization Model for Intersections Experiencing Heavy Scooter–Vehicle Mixed Traffic Flows

Chien-Lun Lan and Gang-Len Chang, *Member, IEEE*

Abstract—In response to the need for designing signal plans for congested intersections caused by heavy scooter–vehicle mixed flows, this paper presents our formulated model for optimizing both the cycle length and signal timings for isolated intersections. The proposed model accounts for the interactions between scooter and vehicle flows and reflects the maneuverability of scooters in the queue formation and discharging process. The robustness of the proposed formulations has been evaluated with field data and laboratory experiments. The signal optimization model, grounded on such formulations for scooter–vehicle mixed flows, has also been implemented at an intersection and assessed with a rigorous before-and-after field analysis. Our research concludes that incorporating the unique properties of scooter flows is essential for design and development of effective signal control strategies to contend with recurrent congestion caused by heavy mixed scooter–vehicle flows.

Index Terms—Mixed scooter–vehicle flows, optimization, traffic signals.

I. INTRODUCTION

CONSIDER a congested intersection experiencing heavy volume of scooter flows, as shown in Fig. 1, where scooters with their flexible maneuverability are often able to filter through vehicle flows and advance to the intersection stop line. Due to the need for less space during either the flow propagation or the formation of standing queues, scooters tend to take advantage of the remaining space between passenger car flows to exercise parallel movements within the same travel lane and to form multiple queues.

This type of urban congestion caused by heavy scooter–vehicle mixed flows is commonly observable in many developing countries, particularly in major Asian cities [1]–[4]. Inadequate public transport systems, coupled with the cost and difficulty in finding parking space, has incentivized more commuters to select the scooter as the primary transportation mode, and consequently caused more chaos to their congested



Fig. 1. Typical approach with scooter–vehicle mixed traffic flows.

urban traffic flows. Hence, how to effectively contend with such urban mixed-flow congestion is the foremost concern of traffic communities in most developing countries. Unfortunately, neither operational guidelines nor design software for tackling such a complex yet imperative issue is available in state-of-the-art literature or state-of-the-practice studies.

Conceivably, one of the essential tasks to address the urban congestion by scooter–vehicle mixed flows is to develop effective tools for design of intersection signal plans and for evaluation of various arterial progression strategies. For the former issue, the core of research is to observe and formulate the interactions between scooter and vehicle flows in the intersection queue formation and discharging process so that one can optimize the signal plan with existing control methodologies. Additional efforts to investigating the interactions and conflicts between vehicle and scooter flows in the arterial propagation process, including car-following and lane-changing behaviors, will be essential for understanding the latter issue and for developing signal progression models.

This paper intends to address the first vital issue of producing a reliable tool for signal design for intersections experiencing heavy scooter–vehicle mixed traffic. The focus of the tool development is to structure a set of convenient yet effective formulations to reflect the interdependent relations between the scooter and vehicle queue lines within a travel lane and account for the interactions within the mixed scooter–vehicle flows in the queue formation and discharging process.

Manuscript received March 22, 2014; revised July 20, 2014 and September 15, 2014; accepted November 12, 2014. This work was supported in part by the Ministry of Transportation and Communications and in part by the National Science Council of Taiwan under Grant 101-2917-I-564-070. The Associate Editor for this paper was J. E. Naranjo.

The authors are with the Department of Civil and Environmental Engineering, University of Maryland, College Park, MD 20742 USA (e-mail: cllan@umd.edu; gang@umd.edu).

Digital Object Identifier 10.1109/TITS.2014.2376292

II. MODELING THE QUEUE FORMATION FOR SCOOTER-VEHICLE MIXED TRAFFIC FLOWS

In review of the related literature, it is noticeable that most existing studies for traffic signal optimization are focused on intersections with mainly passenger car traffic flows. For example, the class of simulation-based methods employed various macroscopic traffic simulation models to capture the vehicle delays and discharging times, which, in turn, serve as the basis for optimizing signal plan [5]–[16]. In contrast, the school of mathematical programming models applied analytical formulations to represent the delays and queues at different stages of signal operations under various traffic demands and then solved the optimal cycle length and timing for each phase with optimization algorithms [17]–[28]. Some other studies, concerning network signal design, also addressed the interrelations between the signal plans and the traveler responses to their route choices [29]–[33]. The large body of such literature, despite their significant contributions in arterial signal control, has not yet addressed any scooter-related traffic issues.

Rather than developing control models, the very scant recent studies on urban scooter traffic issues have focused on investigating the scooter-vehicle mixed flow properties with either microscopic or mesoscopic simulation methods. For example, Arasan and Koshy [34] applied the coordinate-reference method to replicate vehicle-scooter flow movements on a 2-D plane at the microscopic level, and Mathew *et al.* [35] proposed a sublane concept within a travel lane to advance the movement of scooter flows in an arterial. Instead of replicating individual scooters' behavior, some researchers intended to simulate their space needs in exercising longitude and lateral movements using the cellular automaton (CA) model [36], [37]. Since the physical space in a travel lane is conceptually viewed as many equal-size cells in the CA modeling, such simulation models are mesoscopic in nature and need extensive field data for parameter calibration. Some researchers also utilized heterogeneous traffic simulations for describing the level of service in mixed urban traffic flows [38].

Recognizing that understanding the complex scooter-vehicle flow properties remains at the infancy, traffic researchers driven by the design needs have explored the use of passenger car equivalence (PCE) methods, where scooter flows are converted to an equivalent number of passenger cars. Along the same line, some researchers have focused on estimating the PCE values, based on the relationship between traffic stream speed and the resulting mixed-flow density in a link [39]–[41]. For the same purpose, Branston and Zuyleen [42] and Hadiuzzaman *et al.* [43] focused on investigating the impact of scooters on the intersection saturation flow rate and capacity. Several researchers also argued that scooters in the stop queue condition will either increase the start-up lost time of passenger cars or reduce their saturation flow rate [44]–[46]. To circumvent the need to address scooters' dynamic properties, some researchers also adventured the potential of converting passenger cars into scooter equivalent units [47], [48].

Overall, among the limited studies for scooter-vehicle mixed flows, the PCE-based methods remain the most popular practice in design of traffic signals in many developing countries where scooters have emerged as one of the primary transport

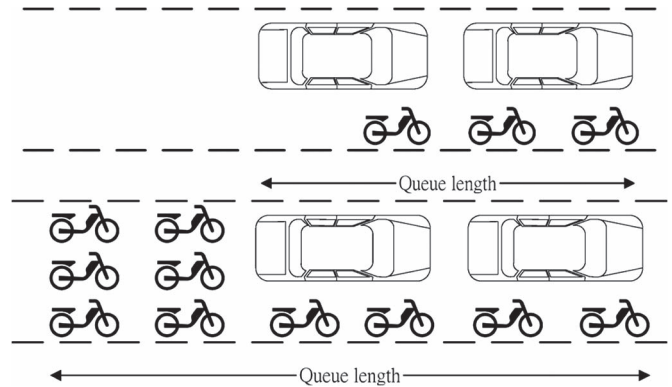


Fig. 2. Queue lengths with various scooter demands.

modes. However, such a convenient conversion method suffers from the lack of rigorous algorithms to estimate the most appropriate PCE that can reliably reflect the actual delays and congestion caused by the target level of mixed scooter-vehicle flows. Moreover, if the congested traffic volume consists of a large share of scooter flows, their conversion to PCEs may result in unrealistically long intersection traffic queues. This is due to the fact that the PCE conversion may reflect, to some extent, the equivalent volume impact from scooters, but cannot capture the maneuverability of scooters that often forms a substantially short queue length from the intersection stop line (see Fig. 2). Failing to account for the impact of scooters on the intersection queue formation and discharging process may significantly overestimate the required green time for signalized intersections and yield an unrealistic bandwidth on the design of arterial progression.

This paper presents our research results on developing a traffic signal optimization model for isolated intersections experiencing heavy scooter-vehicle mixed flows. Unlike existing studies, the proposed signal optimization model explicitly considers the interaction between cars and scooters. By including the large volume of scooter traffic, the model can produce the signal plan that better responds to the needs of scooter-vehicle mixed traffic behavior and yields less traffic delays. The remaining sections are organized as follows. Sections III–V detail the formulations to capture the mixed-flow queue formation and discharging process at an intersection approach, followed by presentation of the signal optimization objective function and solution heuristics in Section VI. Summary of the extensive field assessment and a before-and-after study with our developed model are presented in Section VII. Concluding comments along with future research needs constitute the core of the last section.

III. MODELING THE QUEUE FORMATION OF SCOOTER-VEHICLE MIXED TRAFFIC FLOW

Consider a typical approach with scooter-vehicle mixed traffic flows, as shown in Fig. 1, where each lane can be conceptually divided into sublanes to illustrate scooters' moving and queue behavior with other vehicles. For convenience of model formulations, one can decompose the queue formation process of the scooter-vehicle flows to the intersection stop line

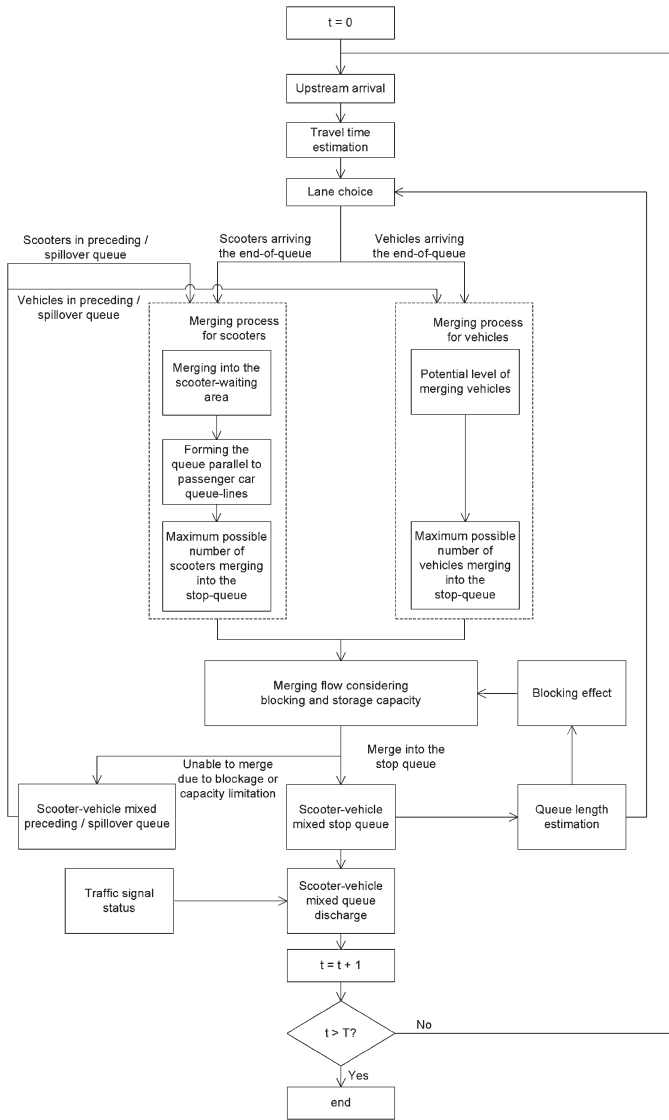


Fig. 3. Flowchart for developing the scooter-vehicle mixed traffic flow model.

into the following consecutive stages: 1) upstream arrival and lane choice; 2) merging into existing queues; and 3) discharge process from the queue line.

Fig. 3 presents the flowchart for scooter-vehicle mixed traffic formulations, grounded on the field-observed information of queue formation and dissipation shown in Fig. 4. The proposed scooter-vehicle model iterates from time index $t = 0$ to the user-defined duration T . The processes for each time step are depicted as follows.

- 1) The model will first calculate the upstream arrival rate, the estimated travel time, and the lane choice of vehicles and scooters to derive their respective arriving rates to join the existing queue.
- 2) The merging process of scooters takes the scooter arriving rates and the number of scooters in the spillover queue as inputs and estimate scooter queue formation as follows: 1) merging into the scooter waiting area; 2) forming the queue parallel to passenger car queue lines; and 3) calculating the maximum possible number of scooters merging into the stop queue.

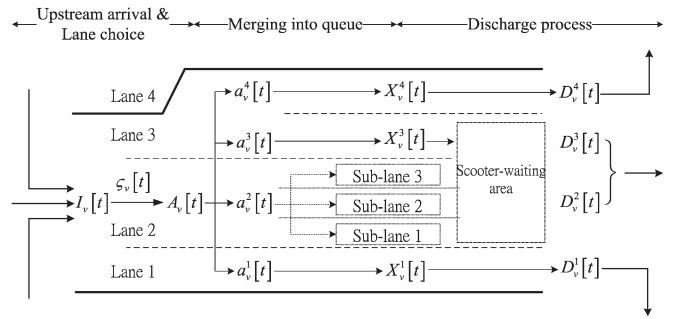


Fig. 4. Graphical illustration of the scooter-vehicle queue formation process at an intersection approach.

 TABLE I
 GEOMETRY AND VEHICULAR PARAMETERS

Variable	Description
ϑ	The length of the target approach
Λ^l	The length of lane l
W^l	The width of lane l
$\Gamma(m)$	The set of lanes serve movement m
E_s	The set of lanes behind the scooter-waiting area
$\gamma_v^m[t]$	The turning ratio toward movement m for type- v vehicles at time step t
$\eta^{m,l}$	The scooters' lane preference factor for lane l serving movement m
\mathcal{X}	The storage space of the scooter-waiting area
u_v	The average traveling speed of type- v vehicles
τ_v	The average length of a type- v vehicle
w_v	The average width of a type- v vehicle
h_v	The average discharge headway of type- v vehicles
O_v	The occupied space of a type- v vehicle
π_v^l	The number of parallel discharging type- v vehicles on lane l
$\tilde{\pi}$	The number of parallel scooters discharging from the scooter-waiting area
$B(l)$	The set of all sub-lanes on lane l
$B_s(l)$	The set of sub-lanes serving scooters forming a queue parallel to car-queue line on lane l

- 3) The merging process for passenger cars and buses consists of two parts: 1) calculate the potential merging vehicles from their arriving rates and the number of vehicles in the spillover queue and 2) calculate the maximum possible number of vehicles merging into the stop queue.
- 4) The number of vehicles merging into the stop queue will be affected by the mutual lane blockage, which is estimated by the queue lengths on all lanes. For those vehicles that cannot merge into the stop queue due to blockage or capacity limitation, they will form as the spillover queues on the neighboring lanes.
- 5) The scooter-vehicle mixed discharge process can be then calculated with the scooter-vehicle mixed queue and the corresponding traffic signal at time t .
- 6) The model iterates to the next time step and stops when it reaches the user-defined duration T .

To facilitate the presentation of the proposed model, some key notations relating to the geometry design and vehicular parameters are listed in Table I; the variables used throughout this paper are also summarized in Table II.

TABLE II
VARIABLE DEFINITIONS

Variable	Description
$I_v[t]$	The entering flow rate of type- v vehicles at the target intersection approach during time step t
$A_v[t]$	The arriving flow rate of type- v vehicles at the end-of-queue on the target intersection approach during time step t
$a_v^l[t]$	The arriving flow rate of type- v vehicles at the end-of-queue on lane l of the target intersection approach during time step t
$P_v^l[t]$	The potential flow rate of type- v vehicles at the end-of-queue on lane l of the target intersection approach during time step t
$M_v^l[t]$	The maximum flow rate of type- v vehicles that may merge into the stop-queue on lane l at time step t
$Q_v^l[t]$	The flow rate of type- v vehicles that joins the queue on lane l at time step t
$q_v^{\beta}[t]$	The flow rate of type- v vehicles that joins the sub-lane β on lane l at time step t
$X_v^l[t], \tilde{X}_v^l[t], \hat{X}_v^l[t]$	The number of type- v vehicles in the stop-queue, the spillover-queue, and the queued behind spillover queue on lane l at time step t
$x_v^{\beta}[t]$	The number of type- v vehicles in the stop-queue on the sub-lane β on lane l at time step t
$S^l[t]$	The average discharge rate of the scooter-vehicle flow on lane l at time step t
$s_v^l[t]$	The discharge rate for type- v vehicles on lane l at time step t
$D_v^l[t]$	The departing flow rate for type- v vehicles on lane l at time step t
$d_v^{\beta}[t]$	The departing flow rate for type- v vehicles from the sub-lane β on lane l at time step t
$\omega_v^l[t]$	The reduced flow rate for type- v vehicles experiencing blockage on lane l at time step t
$\tilde{Q}[t], \bar{D}[t]$	The flow rate of scooters that joins and departs from the scooter-waiting area at time step t
$\tilde{X}[t]$	The number of scooters stopped on the scooter-waiting area at time step t
$\phi^l[t]$	The available space for scooters to queue parallel to passenger car queue on lane l at time step t
$\phi^l[t]$	The number for scooters allowed to queue parallel to passenger car queue on lane l at time step t
$L^l[t]$	The queue length on lane l at time step t
$\bar{L}[t]$	The average queue length across all lanes on the target approach at time step t
$\varsigma_v[t]$	The travel time for type- v vehicles entering the target approach at time step t to reach the end-of-queue
$b^l[t]$	A binary variable describing whether the lane l is blocked or not at time step t
$\tilde{E}[t]$	A binary variable describing whether the scooter-waiting area is empty or not at time step t
$\kappa_v^l[t]$	A binary variable describing whether lane l is blocked by type- v vehicles or not at time step t
Δt	The length of a unit time step
t	The time step index

A. Upstream Arrival and Lane Choice

Let $I_v[t]$ denote the flow rate of type- v vehicles entering from all upstream approaches to the target intersection approach. Then, those vehicles joining the queue, i.e., $A_v[t]$, as shown in Fig. 4, can be expressed as

$$A_v \left[t + \left\lceil \frac{\varsigma_v[t]}{\Delta t} \right\rceil \right] = I_v[t] \quad (1)$$

where $I_v[t]$ is the flow rate of type- v vehicles entering this approach at time step t ; $\varsigma_v[t]$ is their travel time; and $v = 1, 2,$

and 3 represent the scooter, passenger car, and bus, respectively. Since link travel time varies with the speed of each type of vehicles, one can approximate their travel times from entry to join the queue with

$$\varsigma_v[t] = (\vartheta - \bar{L}[t]) \times (u_v)^{-1} \quad (2)$$

where ϑ is the link length, u_v is the average traveling speed of type- v vehicles, and $\bar{L}[t]$ is the average queue length across all lanes at time step t .

As reflected in most field observations, vehicles merging into a lane group (i.e., a set of lanes serving the same turning movement) have a tendency to use the lane exhibiting a shorter queue, and their distributions between queue lanes are generally a function of the existing queue conditions. Hence, one can formulate the distribution of entering scooter-vehicle flows to the available lanes as

$$a_v^l[t] = A_v[t] \times \gamma_v^m[t] \left((L^l[t])^{-1} \times \left(\sum_{l' \in \Gamma(m)} (L^{l'}[t])^{-1} \right)^{-1} \right), \quad l \in \Gamma(m) \quad (3)$$

where $a_v^l[t]$ is the arriving flow rate of type- v vehicles at the end of queue on lane l during the t th time interval, $\gamma_v^m[t]$ is the turning ratio toward movement m for type- v vehicles during the t th time interval, and $L^l[t]$ is the queue length of lane l serving movement m at the time step t . The first two terms of (3) represent the flow rate of vehicles (except for scooters) entering a certain lane group, and the third term is the ratio between the queue length on lane l and the sum of the queue length on all lanes serving the movement m .

Note that, since scooters have a tendency to use the rightmost lane in a lane group, a lane preference factor $\eta^{m,l}$ is thus introduced for scooters' preference, i.e.,

$$a_1^l[t] = A_1[t] \times \gamma_1^m[t] \times \eta^{m,l}. \quad (4)$$

Naturally, the summation of all scooter lane preference factors, serving movement m , shall equal one, that is, $\sum_l \eta^{m,l} = 1$.

In an approach containing a scooter waiting area, (4) should be modified to accommodate the geometry features. For instance, scooters for through movement will merge into a scooter waiting area if the space available for queuing exists. Note that the number of scooters merging into the scooter waiting area will not contribute to the queue formations on each lanes. Hence, let $\check{Q}[t]$ be a variable representing the number of scooters merging into the scooter waiting area, and one can rewrite (4) as

$$a_1^l[t] = \left(A_1[t] \times \gamma_1^m[t] - \check{Q}[t] \right) \times \eta^{m,l}, \quad m = 1 \quad (5)$$

where $\gamma_1^m[t]$ stands for the turning ratio of scooters on movement m at time t ; $m = 1, 2,$ and 3 represent the through, left-turn, and right-turn movements, respectively.

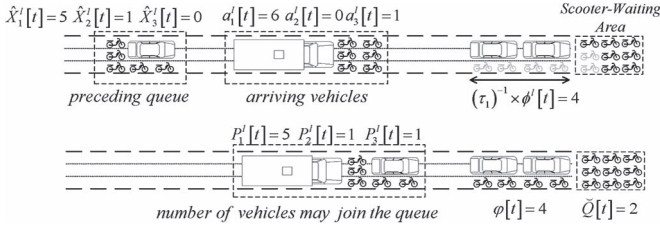


Fig. 5. Graphical illustration of the sublane concept.

B. Merging Into Queues

It is noticeable that the lateral space needed to merge into the queue varies among vehicle types. Since the field data reveal that each typical travel lane is most likely to concurrently accommodate three parallel lines of scooters, this paper thus has divided each lane into three sublanes, as illustrated in Fig. 5, to capture the queue pattern of scooters. Based on the required width for moving and queuing, a bus is assumed to occupy three sublanes, whereas a passenger car and a scooter are assumed to occupy two and one sublanes, respectively.

1) *Merging Process for Scooters:* As scooters arriving at the end of queue on the target approach, their merging behaviors may vary with the encountered queue conditions. For example, these merging behaviors include the following: 1) if the arriving scooters face an empty lane, they will spread equally across all sublanes on the target travel lane; 2) if the arriving scooters approach a lane with some vehicles already stopped in the queue, they will try to merge onto the available spaces between the queue lines formed by passenger cars; and 3) if the number of arriving scooters exceed the available spaces between passenger car queue lines, those overflowed scooters are observed to spread equally across all sublanes on the target lane. Due to the space need of only one sublane, the behavior of the scooters' merging process on a typical passenger car lane can be described with the following three consecutive steps: 1) merging into the scooter waiting area (if such a waiting area exists); 2) forming a queue line in parallel with other vehicles; and 3) joining the queue line behind other stopped vehicles.

Merging into the scooter waiting area: The scooter waiting area (see Fig. 4) is a storage space, exclusively designed for scooters queuing at the stop line to accommodate scooters' high mobility. The scooter waiting areas are often set up across through lanes, as shown in Figs. 1 and 4. Based on field observations, arriving scooters indeed mostly merge into the scooter waiting areas. Once the waiting areas have been fully occupied, scooters will then start to queue on those available travel lanes. Hence, given the storage space of a scooter waiting area, the number of scooters acceptable to merge into the scooter waiting area is set as

$$\check{Q}[t] = \min \left\{ A_1[t] \times \gamma_1^1[t], \chi - \check{X}[t] \right\} \times (1 - g_1[t]) \quad (6)$$

where $\check{X}[t]$ is the number of scooters queued at the scooter waiting area at time t , χ is the storage space of scooter waiting area, and $g_1[t]$ is a binary variable indicating a green phase for the through movement.

Forming the queue lines on a sublane parallel to passenger car queue line (see Fig. 5): For scooters arriving at the end of queue and not able to maneuver to the scooter waiting area, they will form a queue on the shortest sublane within their selected lanes. To estimate the number of scooters forming a queue line parallel to the passenger car queue line, it is necessary to know the available storage space and the number of arriving scooters.

To calculate the space available for scooters to form a queue line parallel to passenger car queue in the same lane, one needs to estimate the existing queue length on each sublane, which is the summation of vehicle lengths multiplied by the number of vehicles in queue by vehicle type, i.e., $\sum_v \tau_v \cdot x_v^{l,\beta}[t]$, where τ_v is the average length of a type- v vehicle, and $x_v^{l,\beta}[t]$ is the number of type- v vehicles in queue on sublane β of lane l at time t .

The available space for scooters to queue on a sublane parallel to passenger car queue, i.e., $\phi^l[t]$, can be approximated with the difference between the maximum queue length among all sublanes and the summation of queue lengths on each sublane. Thus, the available storage space for scooters to form a queue parallel to the queue line for passenger cars on the same lane can be expressed as

$$\phi^l[t] = \max_{\beta} \left(\sum_v \tau_v \cdot x_v^{l,\beta}[t] \right) \times W^l - \sum_{\beta} \sum_v \tau_v \cdot x_v^{l,\beta}[t] \quad (7)$$

where W^l is the number of sublanes on lane l , which is set to 3 in Fig. 5.

Notably, $(\tau_1)^{-1} \times \phi^l[t]$ denotes the number of scooters that can form a queue with the space of $\phi^l[t]$. Since the number of scooters allowed to merge into a sublane, i.e., $\varphi^l[t]$, depends on both the number of scooters arriving from upstream, i.e., $a_1^l[t]$, and scooters already in a queue preceding to spillover queue from neighboring turn bay, i.e., $\hat{X}_1^l[t]$, (which will be simplified as "preceding queue" hereafter), one can show such relations as

$$\varphi^l[t] = \min \left\{ a_1^l[t] + \hat{X}_1^l[t], (\tau_1)^{-1} \times \phi^l[t] \right\}. \quad (8)$$

Joining sublane queues behind other vehicles (see Fig. 5): If the sublane space neighboring to the stopped vehicles cannot accommodate all arriving scooters, the remaining scooters need to mix with other types of vehicles and join the vehicle queue. The number of such scooters can be shown as

$$P_1^l[t] = a_1^l[t] + \hat{X}_1^l[t] - \varphi^l[t] \quad (9)$$

where $a_1^l[t]$ is the number of arriving scooters on lane l during the t th time interval, $\hat{X}_1^l[t]$ is the number of scooters in the preceding queue waiting to merge into lane l at time t , and $\varphi^l[t]$ denotes the number of scooters that form a parallel queue on lane l at time t .

2) *Maximal Possible Number of Vehicles Merging Into a Stop Queue:* Note that the number of vehicles that may join the queue on lane l , denoted by $P_v^l[t]$, includes not only vehicles arriving at the end of queue but also those already in the preceding queue from the last time interval, due to either the

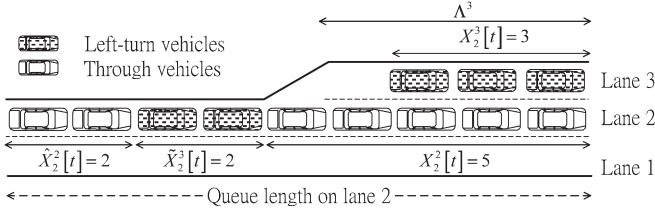


Fig. 6. Graphical illustration of the lane spillover and mutual blockage.

lane blockage (shown as $\hat{X}_v^l[t]$ in Fig. 6, for travel lanes) or spillover from a neighboring turning bay (shown as $\tilde{X}_v^l[t]$, for turn bays).

Hence, the maximal possible number of vehicles that may merge into the queue on lane l at time t can be expressed as

$$P_v^l[t] = a_v^l[t] + \hat{X}_v^l[t], \text{ for travel lanes} \quad (10)$$

$$P_v^l[t] = a_v^l[t] + \tilde{X}_v^l[t], \text{ for turning-bays.} \quad (11)$$

Let the available storage capacity of a lane be the difference between the length of a lane and its standing queue (i.e., $\Lambda^l - L^l[t]$); then, such capacity can be shared by all types of vehicles, based on their share of arriving flow rate ($P_v^l[t]$) in the total arriving flows ($\sum_v P_v^l[t]$). Hence, the maximum flow rate of type- v vehicles, which may merge into the stop queue on lane l , i.e., $M_v^l[t]$, can be expressed as

$$M_v^l[t] = P_v^l[t] \times \left(\sum_{v'} P_{v'}^l[t] \right)^{-1} \times [(\tau_v)^{-1} \times (\Lambda^l - L^l[t])] \quad (12)$$

where τ_v is the average length of a type- v vehicle, Λ^l is the length of lane l , and $L^l[t]$ is the queue length on lane l at time t . The first term shows the proportion of available space shared by each vehicle type, and the second term represents the available queue space on lane l .

IV. BLOCKING EFFECT DUE TO INSUFFICIENT BAY LENGTH

Note that the queue storage space available in each turning lane or bay may not be fully utilized by the arriving scooter-vehicle mixed flow due to the differences in their required physical space and the potentially insufficient bay length.

The mutual blockage may occur when 1) the queue length on a through lane exceeds the entrance of its adjacent turning bay and 2) the queue vehicles on a turning bay have spilled over their storage space and thus block vehicles on the neighboring lane. Those that could not merge into their target turning bays upon arrival are called spillover queues, i.e., $\tilde{X}_v^l[t]$, where some later arriving through vehicles, i.e., $\hat{X}_v^l[t]$, are often blocked by such spillover queues during their designated discharging time, thus forming a second batch of queue line behind the spillover queue.

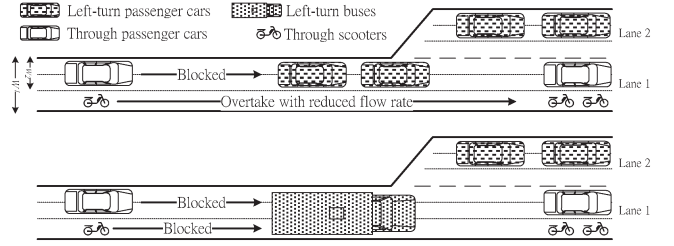


Fig. 7. Blocking effects of passenger cars and scooters.

Fig. 6 illustrates the blockage to left-turn vehicles caused by the through queue traffic. The binary variable, i.e., $b^l[t]$, is used to denote if a lane is blocked at time t , i.e.,

$$b^l[t] = \begin{cases} 1, & \text{if } L^{l'}[t] > \Lambda^{l'} \text{ and lane } l' \text{ is adjacent to lane } l \\ 0, & \text{otherwise.} \end{cases} \quad (13)$$

In summary, the queue length on a lane actually consists of three types of queue vehicles: 1) stop queues; 2) vehicles stopped behind vehicles spilling over from adjacent lanes; and 3) spillover queues from the adjacent lanes. Therefore, the actual queue length on a target lane can be estimated with the following expression:

$$L^l[t] = \max_{\beta} \left(\sum_v \tau_v \cdot x_v^{l,\beta}[t] \right) + \sum_v (\pi_v^l)^{-1} \cdot \tau_v \cdot \hat{X}_v^l[t] + \sum_v (\pi_v^l)^{-1} \cdot \tau_v \cdot \tilde{X}_v^l[t]. \quad (14)$$

The first term in (14) represents the length of the vehicles in the stop queues, the second term estimates the length of vehicles queued behind vehicles spilling over from the adjacent lanes, whereas the third term reflects the length of spillover queues from the adjacent lanes.

A. Blocking Impacts by Different Types of Vehicles

Different from passenger cars, scooters prior to join the vehicle queue line often intend to take advantage of available sublane space parallel to the existing queue line, as shown in Fig. 7. However, under the typical lane width of 3.6 m (12 ft), a spillover bus is observed to completely block the arriving vehicles from merging into the available downstream space. In contrast, a queuing passenger car, about 2 m wide, may completely block the arriving cars and buses, but can only partially block the arriving scooters. To reflect such blockage impacts, let the lane width be denoted by W^l and the width of a type- v vehicle be assumed as w_v . Then, the reduction in the flow rate for those overtaking scooters will be w_v/W^l , where a bus is assumed to block the scooters completely. Equation (15) uses a simple binary indicator to define the blockage status of a given lane, i.e.,

$$\kappa_v^l[t] = \begin{cases} 1, & \text{if } \tilde{X}_v^l[t] \geq 0 \\ 0, & \text{otherwise} \end{cases} \quad (15)$$

where $\kappa_v^l[t]$ denotes whether lane l is blocked by type- v vehicles or not.

Therefore, the reduced flow rate for scooters due to a lane blockage can be then calculated as

$$\omega_1^l[t] = \min \left\{ \sum_{v=2,3} w_v \times (W^l)^{-1} \times \kappa_v^l[t], 1 \right\}. \quad (16)$$

As for other vehicle types, no overtaking is possible when blockage occurs. The reduced flow rate can be computed with the following expression:

$$\omega_v^l[t] = \min \{ \kappa_2^l[t] + \kappa_3^l[t], 1 \}, \quad v = 2 \text{ and } 3. \quad (17)$$

B. Queue Formation Considering the Storage Space Limitation and Blocking Effect

Conceivably, the actual vehicle flows to form the queue on a lane should depend on the following: 1) the arriving distribution of different types of vehicles and 2) the presence of lane blockages. Hence, the total number of type- v vehicles joining the queue on lane l at time step t is given by

$$Q_v^l[t] = \min \{ P_v^l[t], M_v^l[t] \} \times (1 - \omega_v^l[t] \times b^l[t]) \quad (18)$$

where the first term gives the maximum merging flow due to storage limitation, and the second term considers the reduced flow rate due to lane blockage.

The arriving scooters to queue behind existing vehicle queue line are assumed to spread across all sublanes, as shown in

$$q_1^{l,\beta}[t] = (\pi_1^l)^{-1} \times Q_1^l[t]. \quad (19)$$

Note that either passenger car or bus flows will form a single queue on each lane following a typical queue-flow pattern. Moreover, those arriving vehicles, which cannot merge into their target turn bay and spill over to a neighboring lane, can be shown as

$$\tilde{X}_v^l[t+1] = (P_v^l[t] - Q_v^l[t]) \cdot \Delta t, \quad \text{if } l \text{ is a turning-bay} \quad (20)$$

where $P_v^l[t]$ is the number of vehicles that may join the queue on turn bay l at time t , and $Q_v^l[t]$ is the number of vehicles that actually join the queue.

As for vehicles forming a queue line behind those spillover vehicles, they can be approximated as

$$\hat{X}_v^l[t+1] = (P_v^l[t] - Q_v^l[t]) \cdot \Delta t, \quad \text{if } l \text{ is a turning-lane.} \quad (21)$$

V. DISCHARGE PROCESS

The discharge process in scooter-vehicle mixed flows differs significantly from vehicle-only scenarios. First, scooters often do not follow the lane discipline and often drive in parallel with other vehicles. Second, traffic queues on those lanes connected to the scooter waiting area will discharge after those scooters in the scooter waiting areas. Hence, scooters, depending on the location they choose to stop, may discharge both concurrently or sequentially with other vehicles.

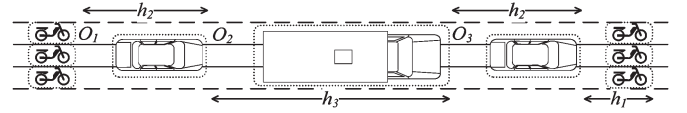


Fig. 8. Graphical illustration of the discharging process.

A. Discharge Process in the Scooter Waiting Area

Scooter waiting areas include only scooter flows, which allows several rows of scooters to concurrently discharge in parallel at the onset of the green phase. One can thus show the discharge flow rate of scooters in this area as

$$\check{D}[t] = \min \left\{ \check{Q}[t] \cdot \Delta t + \check{X}[t], (\tilde{\pi})^{-1} \times (h_1)^{-1} \times g_1[t] \right\} \times (\Delta t)^{-1} \quad (22)$$

where $\tilde{\pi}$ is the number of parallel scooters discharging from the scooter waiting area, h_1 is the average discharge headway of scooters, and $g_1[t]$ is a binary variable indicating if the through movement is given the green phase or not at time step t .

Therefore, for scooter queues on a scooter waiting area, the flow conservation can be formulated as

$$\check{X}[t+1] = \check{X}[t] + (\check{Q}[t] - \check{D}[t]) \cdot \Delta t. \quad (23)$$

B. Discharge Process for a Lane of Mixed Flows

Note that, due to the discrepancy in the occupied space and operational features (e.g., discharge headways and parallel driving rows), the discharge flow rate varies between different vehicle types, where scooters certainly have the highest discharge rate. To account for the green time needed to discharge the traffic flows having multiple vehicle types, this paper proposes the use of a mixed discharge rate, weighted with the number of each type of vehicles in the queue. Fig. 8 illustrates the discharging process of scooter-vehicle mixed flows, where O_v represents the occupied space of a type- v vehicle, h_v denotes the average discharge time lag following a type- v vehicle, and π_v^l is the number of parallel driving lines for type- v vehicles.

More specifically, considering the difference in discharge headways, occupied space, number of vehicles in queue, and parallel driving behavior, one can approximate the average discharge rate of the scooter-vehicle flow, i.e., $S^l[t]$, with

$$S^l[t] = \left(\frac{\sum_v X_v^l[t] \cdot \pi_v^l \cdot h_v \cdot O_v}{\sum_v X_v^l[t] \cdot O_v} \right)^{-1} \quad (24)$$

where π_v^l is the number of parallel discharging type- v vehicles on lane l , h_v is the average discharge headway of a type- v vehicle, O_v is the occupied space of a type- v vehicle, and $X_v^l[t]$ is the number of type- v vehicles in queue on lane l at time step t .

Giving the preceding mixed-flow discharge rate, the actual discharge rate during the green phase for each vehicle type is

assumed to be proportional to its ratio in the total scooter-vehicle mixed flow and can be shown as

$$s_v^l[t] = S^l[t] \times \left(X_v^l[t] \times \left(\sum_{v'} X_{v'}^l[t] \right)^{-1} \right) \quad (25)$$

where $s_v^l[t]$ is the discharge rate for type- v vehicles on lane l at time step t .

Since the total vehicle demand to the target intersection approach is the summation of vehicles joining the queue, i.e., $Q_v^l[t]$, and those already in the queue, i.e., $X_v^l[t]$, the actual departing flow rate from lane l at time step t shall be expressed as

$$D_v^l[t] = \min \{ Q_v^l[t] \cdot \Delta t + X_v^l[t], s_v^l[t] \times g_m[t] \} \\ \times (\Delta t)^{-1}, \quad l \notin E_s \quad (26)$$

where $g_m[t]$ is a binary variable indicating a green phase for the movement m served by lane l , and lane l is not affected by the scooter waiting area.

However, for those lanes affected by the scooter waiting area, denoted by E_s , (26) needs to be further modified as shown in

$$D_v^l[t] = \min \{ Q_v^l[t] \cdot \Delta t + X_v^l[t], s_v^l[t] \times g_m[t] \} \\ \times (\Delta t)^{-1} \times \check{E}[t], \quad l \in E_s \quad (27)$$

where $\check{E}[t]$ is a binary variable indicating whether the scooter waiting area is empty or not at time step t , i.e.,

$$\check{E}[t] = \begin{cases} 1, & \text{if } \check{X}[t] = 0 \\ 0, & \text{otherwise.} \end{cases} \quad (28)$$

Note that the total number of scooters can be discharged from a lane equal the summation of scooters discharging from all sublanes. It is assumed that the distribution of the discharge rate among all sublanes is based on their respective scooters in the queue, which can be formulated as

$$d_1^{l,\beta}[t] = \left(x_1^{l,\beta}[t] \times \left(\sum_{\beta'} x_1^{l,\beta'}[t] \right)^{-1} \right) \times D_1^l[t]. \quad (29)$$

By considering the merging and discharging flow rates, the number of scooters in queue on a sublane can be updated as

$$x_v^{l,\beta}[t+1] = x_v^{l,\beta}[t] + (q_v^{l,\beta}[t] - d_v^{l,\beta}[t]) \cdot \Delta t, \quad \text{for } \beta \in B(l) \setminus B_s(l) \quad (30)$$

where $B(l)$ is the set of all sublanes on lane l , and $B_s(l)$ is the set of sublanes serving scooters forming a queue parallel to car queue line on lane l .

However, since scooters may form a queue on a sublane parallel to the passenger car queue line, one needs to add an additional term to (30) as

$$x_1^{l,\beta}[t+1] = x_1^{l,\beta}[t] + (q_1^{l,\beta}[t] + \varphi^l[t] - d_1^{l,\beta}[t]) \cdot \Delta t, \\ \text{for } \beta \in B_s(l) \quad (31)$$

where $\varphi^l[t]$ is the number of scooters that merge into sublane β parallel to other stopped vehicles on lane l at time step t .

VI. SIGNAL OPTIMIZATION MODEL AND SOLUTION HEURISTICS

A. Objective Function

The primary objective of the signal optimization model, as shown in (32), is to minimize the total queue delays in the controlled area within a given time period, i.e.,

$$\min \sum_i \sum_t \left(\sum_v \sum_l (X_v^{i,l}[t] + \check{X}_v^{i,l}[t] + \hat{X}_v^{i,l}[t]) + \check{X}^i[t] \right) \cdot \Delta t \quad (32)$$

where i denotes the index of intersection approaches. Standard equations, representing the signal operation constraints, are shown in

$$C \geq C_{\min}, \quad C \leq C_{\max} \quad (33)$$

$$G^p \geq G_{\min}^p, \quad G^p \leq C \quad \forall p \quad (34)$$

$$\sum_p G^p + I^p = C. \quad (35)$$

Equation (33) ensures the cycle length, i.e., C , to lie between the given minimum, i.e., C_{\min} , and maximum, i.e., C_{\max} , cycle lengths. Equation (34) indicates that the green time for phase p should be more than the given minimum green time, i.e., G_{\min}^p , but less than the cycle length. The condition that the summation of phase durations and interphase lost times, i.e., I^p , should equal the cycle length is guaranteed in (35). The phase status utilized in formulating traffic evolution can be generated with

$$g^p[t] = \begin{cases} 1, & \text{if } \sum_{j=1}^{p-1} (G^j + I^j) < \text{mod}(t, C) \\ & \leq \sum_{j=1}^{p-1} (G^j + I^j) + G^p \\ 0, & \text{otherwise} \end{cases} \quad (36)$$

$$g_m[t] = g^p[t] \times \Psi_m^p \quad (37)$$

where (36) determines the value for binary variable $g^p[t]$, which is used to indicate whether it is phase p or not at time t ; $g^p[t]$ is multiplied by a given phase-movement incidence matrix, i.e., Ψ_m^p , to show the green time for each movement $g_m[t]$.

In summary, the signal optimization model for an intersection with heavy scooter flows can be recapitulated as

$$\min \sum_i \sum_t \left(\sum_v \sum_l (X_v^{i,l}[t] + \check{X}_v^{i,l}[t] + \hat{X}_v^{i,l}[t]) + \check{X}^i[t] \right) \cdot \Delta t$$

s.t. Equations (1)–(31) and (33)–(37).

B. Solution Heuristics

Since the proposed signal optimization model consists of nonlinear constraints and binary variables, it is naturally more efficient to develop proper heuristics to generate solutions. The idea behind the heuristics is to provide a set of signal timings, which satisfies traffic demands from each approach

under undersaturated conditions. To do so, an iterative method, which aims to eliminate residual queues on all intersection approaches with the optimal green timing allocation for each phase, is proposed as follows.

Step 1: Initialization

— Given the initial timing plan

$$\text{Set } G^p = G_{\min}^p \quad C = \sum_p G^p + I^p. \quad (38)$$

Step 2: Estimate the traffic evolution with the scooter–vehicle mixed traffic model.

— Estimate the residual queues for each movement, i.e., $R_{m,v}$, in each approach with the underlying traffic evolution models, that is, (1)–(31), (36), and (37).

Step 3: Calculate the signal improvement direction.

— Estimate the average discharge rate for type- v vehicles on a movement, i.e., $\bar{s}_{m,v}$, by

$$\bar{s}_{m,v} = \sum_t \sum_l s_v^l[t] \times g_m[t] \times \left(\sum_t g_m[t] \right)^{-1} \quad \forall l \in \Gamma(m). \quad (39)$$

— Estimate the additional green time, i.e., \tilde{g}_m , for the need of all vehicle types on a movement by

$$\tilde{g}_m = \max_v \{ R_{m,v} \times (\bar{s}_{m,v})^{-1} \}. \quad (40)$$

— Set the length of an increment for green time for a phase by

$$\tilde{G}^p = \max_m \{ \tilde{g}_m \}, \quad \forall \text{ movement } m \text{ served by phase } p. \quad (41)$$

Step 4: Stopping rule

— If 1) $\tilde{G}^p = 0$ or 2) $\tilde{C} = \sum_p (G^p + \tilde{G}^p) + I^p \geq C_{\max}$, stop and output the signal timings, i.e., G^p . If not, continue to step 5.

Step 5: Update signal timings

— Update the signal timing by $G^p = G^p + \tilde{G}^p$ and $C = \sum_p G^p + I^p$; go to step 2.

VII. EVALUATION OF THE PROPOSED FORMULATIONS WITH FIELD DATA

Since the effectiveness of the proposed optimization model for scooter–vehicle mixed flows hinges on the reliability of the underlying formulations for queue formation and discharge, this paper has conducted several evaluations with field data. The first assessment compares the cumulative throughputs per lane and per vehicle type between the field-observed and model-produced results, whereas the second comparison shows the discrepancy of the queue evolution process reflected in the actual data and the model's output. The results of those two comparisons with field data offer the basis to assess the applicability of the proposed model. The proposed model has

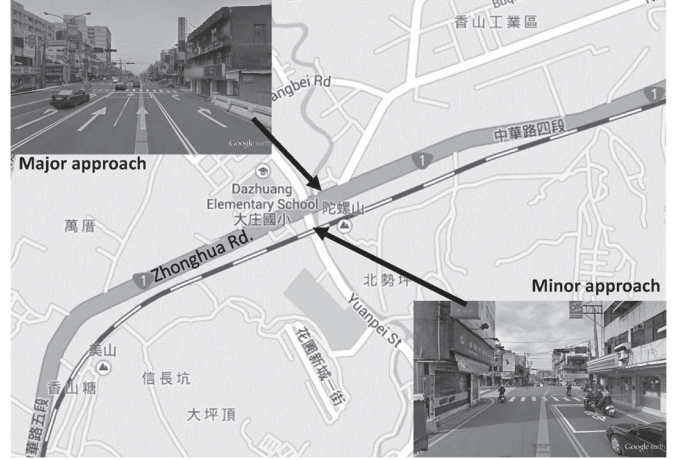


Fig. 9. Survey site.

been also implemented at an intersection for a before-and-after performance comparison.

A. Evaluation of the Per-Lane Cumulative Throughputs

Fig. 9 shows the field site, where the target approach includes one right-turn lane (150M), two through lanes (150M), and one left-turn bay (35M). A scooter waiting area is present preceding the two through lanes.

The data were collected on November 7, 2013, between 04:00 P.M. and 05:00 P.M. with two camcorders mounted over the target approach. The per-lane and per-vehicle-type traffic counts are aggregated in intervals of 5 min, as shown in Table III. The total volume consists of 1325 vehicles, of which 41.4% are scooters, 55.8% are passenger cars, and 2.8% are buses. The signal phases for the target approach are shown in Fig. 10, where the cycle length is 140 s, and the green times of those phases are set as 60, 30, and 50 s, respectively.

Fig. 11 shows the cumulative throughputs between the model and the field data. Table IV recapitulates the difference between the model-produced and the field-observed cumulated throughputs. The overall difference in percentage across all lanes is summarized in the last row.

Notably, the differences between the total scooter throughputs by the model and from the field data fall between 8 and -5 , given the total scooter throughput of 549. The same comparison results lie within the range of 4 and -12 out of the total throughput of 739 passenger cars. It should be mentioned that the discrepancy falls between 6 and -9 for the bus throughput is relatively high, which is inevitable due to its very small volume. Overall, the results of throughput comparison show that the proposed formulations for scooter–vehicle mixed flows can reasonably reflect the actual traffic conditions.

B. Queue Formation and Discharging Process

Queue lengths and clearance times are the most critical parameters for design of a signal plan. The evaluation compares the field collected queue lengths and queue clearance times with those from the proposed model. The field data were collected by a video camera over a four-lane arterial, as shown

TABLE III
DISTRIBUTION OF TRAFFIC COMPOSITION FROM THE FIELD DATA

Time	Left-turn			Through Lane 1			Through Lane 2			Right-turn		
	Scooter	Car	Bus	Scooter	Car	Bus	Scooter	Car	Bus	Scooter	Car	Bus
16:00	14	6	1	0	21	0	29	25	0	13	0	0
16:05	7	5	0	1	27	0	23	23	0	22	3	0
16:10	10	12	0	0	36	0	9	31	1	12	7	1
16:15	7	10	0	0	22	2	23	25	4	16	2	0
16:20	8	10	2	0	20	1	18	17	4	11	1	0
16:25	12	10	1	1	25	0	9	24	3	8	8	0
16:30	21	7	1	1	25	0	18	31	0	11	10	0
16:35	12	7	1	0	23	0	17	20	1	16	6	0
16:40	9	13	0	5	29	0	33	23	2	11	6	0
16:45	13	17	2	1	23	0	21	20	2	8	9	0
16:50	14	6	1	1	20	3	14	18	2	6	7	0
16:55	12	10	0	3	21	0	41	15	2	8	3	0
Total	139	113	9	13	292	6	255	272	21	142	62	1

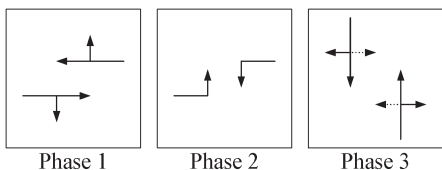


Fig. 10. Phasing design for the target intersection.

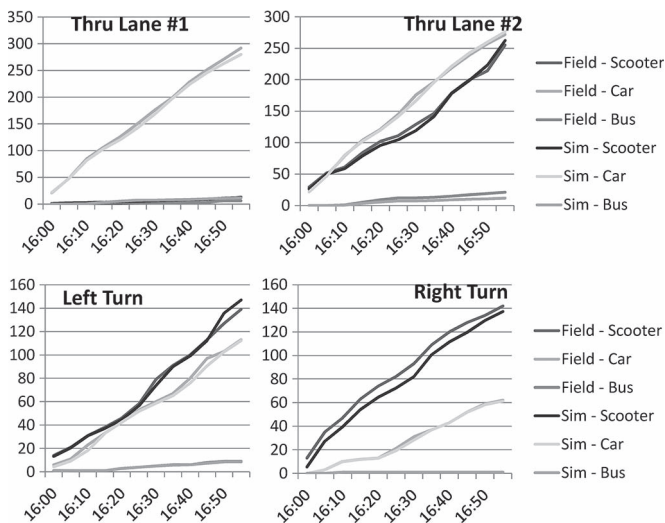


Fig. 11. Model-produced versus field-observed cumulated throughputs.

in Fig. 12. The lanes are numbered from the leftmost lane toward the rightmost lane. A scooter waiting area is present preceding two rightmost lanes. The stop queue length and the number of arriving and departing vehicles are recorded in a per-second basis for comparison. The vehicles initially in queue are reported in Table V.

As shown in Fig. 13, the general shape of the model output and the field data are sufficiently close. The queue length estimated with the proposed formulations for scooter-vehicle flows is compared with field data and reported in Table V, which confirms the promising features of the proposed model for field applications. The queue lengths estimated by PCEs (ranging

from 0.15 to 0.35) are also listed in Table V. It is noticeable that using a PCE-based conversion method may yield unrealistic long queues for those scenarios with high volumes of scooters.

C. Field Applications With the Scooter-Vehicle Mixed Flow Model

The proposed signal optimization model has been implemented at an intersection with the signal phasing shown in Fig. 10. Traffic volumes were collected on November 7 during the peak hours (05:00 P.M. to 06:00 P.M.), and the total traffic volume was about 5876 vehicles, of which 67.4% are scooters, 30.6% are passenger cars, and 2% are buses (see Table VI). The resulting signal timings based on the field data are shown in Table VII.

The total traffic demand on November 12, for the after survey, was around 5876 vehicles, but with different flow ratios. Among them, 65.8% are scooters, 32.4% are passenger cars, and 1.8% are buses. Delays at each approach were collected with two camcorders mounted over the approach and one camcorder at the upstream entrance of the approach. The before-and-after comparison per approach delay with respect to vehicle type is reported in Table VIII. The results show a reduction of 39.2% in the total delay, except for buses due to its very small volume.

VIII. CONCLUSION

This paper has presented an optimization model for design of intersection signal timings under heavy scooter-vehicle mixed traffic flows. To capture the spatial interactions between scooters and vehicles, this paper has proposed a set of formulations to reflect the queue formation and discharging process at intersection approaches. Our extensive investigation results confirm that the proposed model can yield realistic estimates of throughputs, queue lengths, and queue clearance times for the mixed traffic flows. A field implementation at an intersection of heavy scooter flows and the before-and-after comparison also confirmed the effectiveness of the proposed model.

TABLE IV
DIFFERENCES BETWEEN THE MODEL-PRODUCED AND FIELD-OBSERVED CUMULATED THROUGHPUTS

Time	Left-turn			Through Lane 1			Through Lane 2			Right-turn		
	Scooter	Car	Bus	Scooter	Car	Bus	Scooter	Car	Bus	Scooter	Car	Bus
16:00	-1	-2	0	1	1	0	-3	-4	0	-8	0	0
16:05	0	-2	0	1	0	0	-2	-1	0	-8	0	0
16:10	0	-5	0	2	-3	0	-2	1	-1	-8	0	0
16:15	-1	0	0	3	-3	1	-5	-2	-2	-9	0	0
16:20	-1	0	0	3	-5	3	-7	-1	-3	-9	0	0
16:25	-2	-1	0	3	-8	4	-7	-3	-5	-10	-2	0
16:30	-5	-1	0	3	-8	4	-10	-9	-5	-11	-3	0
16:35	-1	-2	0	4	-2	5	-5	-1	-5	-8	0	0
16:40	-1	-4	0	0	-4	6	-1	3	-6	-8	0	0
16:45	-1	-6	-1	1	-5	7	-1	4	-7	-8	0	0
16:50	9	0	-1	1	-8	5	9	3	-8	-4	-1	0
16:55	8	-1	-1	0	-12	6	7	4	-9	-5	-1	0
Cumulated Error	5.8%	-0.9%	-11.1%	0	-4.1%	100%	2.7%	1.5%	-42.9%	-3.5%	-1.6%	0



Fig. 12. Site for field observations of the queue formation and discharging process.

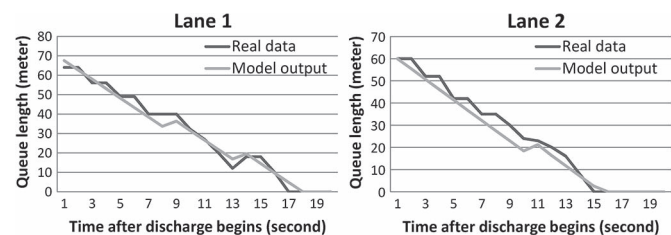


Fig. 13. Comparison of queue length between the model output and the field results.

TABLE V
NUMBER OF VEHICLES AND QUEUE LENGTH PRIOR TO THE DISCHARGE PROCESS

Type	Scooter-waiting area	Lane 1	Lane 2	Lane 3	Lane 4
Scooters (veh)	16	3	7	31	46
Cars (veh)	0	9	8	7	4
Actual queue length (m)	N.A.	64	60	60	40
Estimated queue length (m)	N.A.	67.5	60	59.7	37.6
Proposed model Estimated queue length (m)	N.A.	71	74	127	143
PCE = 0.35					
Estimated queue length (m)	N.A.	69	70	105	110
PCE = 0.25					
Estimated queue length (m)	N.A.	67	64	83	77
PCE = 0.15					
Real queue clearance time (s)	N.A.	16	14	17	16
Estimated queue clearance time (s)	N.A.	17	15	19	15

Future extensions along the same line shall include formulations of the scooter-vehicle flow propagation along a link and development of arterial progression models for traffic flows with a high percentage of scooters. The impact of high bus flows on the propagation of the scooter-vehicle mixed flows should be also a vital research subject.

TABLE VI
TRAFFIC DEMANDS AT THE TARGET INTERSECTION (NOVEMBER 7, 2013)

Approach	Turning	Scooters	Cars	Buses	Summation
Westbound	Left	190	109	8	307
	Through	781	558	54	1,393
	Right	232	83	6	321
Eastbound	Left	56	55	4	115
	Through	584	507	22	1,113
	Right	76	53	1	130
Southbound	Left	136	44	1	181
	Through	548	58	2	608
	Right	85	57	4	146
Northbound	Left	171	42	1	214
	Through	605	80	1	686
	Right	495	154	13	662
Total		3,959	1,800	117	<u>5,876</u>

TABLE VII
ORIGINAL SIGNAL PLAN AND MODEL OUTPUT

Type	Cycle Length	Phase 1	Phase 2	Phase 3
Original Timing (s)	140	60	30	50
Model Output (s)	140	55	20	65

ACKNOWLEDGMENT

The authors would like to thank Dr. H.-J. Cho for his constructive suggestions during the entire research. They would

TABLE VIII
BEFORE-AND-AFTER COMPARISON OF
PER VEHICLE DELAY, PER APPROACH

	Before (Nov. 7)			After (Nov. 12)		
	Scooters	Cars	Buses	Scooters	Cars	Buses
Westbound	10.7	18.4	4.7	10.2	20.5	20.6
Eastbound	26.1	28.9	60.1	24.9	29.5	26.5
Southbound	14.1	46.3	48	8.1	19.8	34
Northbound	48.3	56.7	49.5	12.9	18.4	14
Total Delay	161,397 (veh-s)			98,072 (veh-s)		

also like to thank the transportation team members of National Chiao Tung University and National Taiwan University for collection and preliminary documentation of field data.

REFERENCES

- [1] P. A. Barter, "Urban transport in Asia: Problems and prospects for high-density cities," *Asia-Pac. Develop. Monit.*, vol. 2, no. 1, pp. 33–66, 2000.
- [2] T. P. Hsu, A. F. Mohd Sadullah, and X. D. Nguyen, "A comparative study on motorcycle traffic development of Taiwan, Malaysia and Vietnam," *J. East. Asia Soc. Transp. Stud.*, vol. 5, pp. 381–395, 2003.
- [3] L. V. Leong and A. F. Mohd Sadullah, "A study on the motorcycle ownership: A case study in Penang State, Malaysia," in *Proc. Eastern Asia Soc. Transp. Stud.*, 2007, vol. 7, pp. 528–239.
- [4] A. S. Almselati, R. A. Rahmat, and O. Jaafar, "An overview of urban transport in Malaysia," *Soc. Sci.*, vol. 6, no. 1, pp. 24–33, 2011.
- [5] D. I. Robertson, "TRANSYT: A traffic network study tool," Road Res. Lab., Berkshire, U.K., LR-253, 1969.
- [6] G. C. D'ans and D. C. Gazis, "Optimal control of oversaturated store- and forward transportation networks," *Transp. Sci.*, vol. 10, no. 1, pp. 1–19, Feb. 1976.
- [7] N. H. Gartner, "OPAC: A demand-responsive strategy for traffic signal control," *Transp. Res. Rec.*, vol. 906, pp. 75–81, 1983.
- [8] D. I. Robertson and R. D. Bretherton, "Optimizing networks of traffic signals in real time—The SCOOT method," *IEEE Trans. Veh. Technol.*, vol. 40, no. 1, pp. 11–15, Feb. 1991.
- [9] *TRANSYT-7F User Manual*, Federal Highway Administration, Washington, DC, USA, 1991.
- [10] M. Papageorgiou, "An integrated control approach for traffic corridors," *Transp. Res. C, Emerging Technol.*, vol. 3, no. 1, pp. 19–30, Feb. 1995.
- [11] S. C. Wong, "Group-based optimization of signal timings using the TRANSYT traffic model," *Transp. Res. B, Methodol.*, vol. 30, no. 3, pp. 217–244, Jun. 1996.
- [12] P. Mirchandani and L. Head, "A real-time traffic signal control system: Architecture, algorithms, analysis," *Transp. Res. C, Emerging Technol.*, vol. 9, no. 6, pp. 415–432, Dec. 2001.
- [13] T. H. Chang and G. Y. Sun, "Modeling and optimization of an oversaturated signalized network," *Transp. Res. B, Methodol.*, vol. 38, no. 8, pp. 687–707, Sep. 2004.
- [14] *TRANSYT 14 User Guide*, TRL Software, Wokingham, U.K., 2010.
- [15] Y. Liu and G. L. Chang, "An arterial signal optimization model for intersections experiencing queue spillback and lane blockage," *Transp. Res. C, Emerging Technol.*, vol. 19, no. 1, pp. 130–144, Feb. 2011.
- [16] Y. Y. Chen and G. L. Chang, "A macroscopic signal optimization model for arterials under heavy mixed traffic flows," *IEEE Trans. Intell. Transp. Syst.*, vol. 15, no. 2, pp. 805–817, Apr. 2014.
- [17] R. E. Allsop, "Estimating the traffic capacity of a signalized road junction," *Transp. Res.*, vol. 6, no. 3, pp. 245–255, Sep. 1972.
- [18] N. H. Gartner, J. D. C. Little, and H. Gabbay, "Optimization of traffic signal setting by mixed-integer linear programming, Part I: The network coordination problem," *Transp. Sci.*, vol. 9, no. 4, pp. 321–343, Nov. 1975.
- [19] N. H. Gartner, J. D. C. Little, and H. Gabbay, "Optimization of traffic signal setting by mixed-integer linear programming, Part II: The network synchronization problem," *Transp. Sci.*, vol. 9, no. 4, pp. 344–363, Nov. 1975.
- [20] N. H. Gartner, S. F. Assmann, F. L. Lasaga, and D. Hou, "A multi-band approach to arterial traffic signal optimization," *Transp. Res. B, Methodol.*, vol. 25, no. 1, pp. 55–74, Feb. 1991.
- [21] J. D. C. Little, M. D. Kelson, and N. H. Gartner, "MAXBAND: A program for setting signals on arterials and triangular networks," *Transp. Res. Rec.*, vol. 795, pp. 40–46, 1999.
- [22] B. G. Heydecker and I. W. Dudgeon, "Calculation of signal settings to minimise delay at a junction," in *Proc. 10th Int. Symp. Transp. Traffic Theory*, 1987, pp. 159–178.
- [23] C. K. Wong and S. C. Wong, "A lane-based optimization method for minimizing delay at isolated signal-controlled junctions," *J. Math. Model. Algorith.*, vol. 2, no. 4, pp. 379–407, Dec. 2003.
- [24] C. K. Wong and S. C. Wong, "Lane-based optimization of signal timings for isolated junctions," *Transp. Res. B, Methodol.*, vol. 37, no. 1, pp. 63–84, Jan. 2003.
- [25] C. K. Wong, S. C. Wong, and C. O. Tong, "A lane-based optimization method for the multi-period analysis of isolated signal-controlled junctions," *Transportmetrica*, vol. 2, no. 1, pp. 53–85, Jan. 2009.
- [26] R. E. Allsop, "SIGSET: A computer program for calculating traffic capacity of signal-controlled road junctions," *Traffic Eng. Control*, vol. 12, pp. 58–60, 1971.
- [27] R. E. Allsop, "SIGCAP: A computer program for assessing the traffic capacity of signal-controlled road junctions," *Traffic Eng. Control*, vol. 17, pp. 338–341, 1976.
- [28] G. Improta and G. E. Cantarella, "Control systems design for an individual signalized junction," *Transp. Res. B, Methodol.*, vol. 18, no. 2, pp. 147–167, Apr. 1984.
- [29] R. E. Allsop, "Some possibilities for using traffic control to influence trip destinations and route choice," in *Proc. 6th Int. Symp. Transp. Traffic Theory*, 1974, pp. 345–374.
- [30] N. H. Gartner, "Area traffic control and network equilibrium," in *Proc. Lect. Notes Econ. Math.*, 1976, vol. 118, pp. 274–297.
- [31] G. E. Cantarella, G. Improta, and A. Sforza, "A procedure for equilibrium network traffic signal setting," *Transp. Res. A, Gen.*, vol. 25, no. 5, pp. 241–249, Sep. 1991.
- [32] F. A. Marciano, G. Musolino, and A. Vitetta, "Signal setting optimization with route choice behavior and acyclic profiles of vehicular flows in road networks," *Procedia Social Behav. Sci.*, vol. 54, pp. 1330–1338, Oct. 2012.
- [33] G. E. Cantarella, P. Velonà, and A. Vitetta, "Signal setting with demand assignment: Global optimization with day-to-day dynamic stability constraints," *J. Adv. Transp.*, vol. 46, no. 3, pp. 254–268, Jul. 2012.
- [34] V. T. Arasan and R. Z. Koshy, "Methodology for modeling highly heterogeneous traffic flow," *J. Transp. Eng.*, vol. 131, no. 7, pp. 544–551, Jul. 2005.
- [35] T. V. Mathew, C. R. Munigety, A. Cherian, and A. Ostawal, "A space discretization based simulation approach for non-lane based traffic conditions," presented at the Transportation Research Board 93rd Annual Meeting, Washington, DC, USA, Jan. 12–16, 2014, Paper 14-3854.
- [36] L. W. Lan and C. W. Chang, "Inhomogeneous cellular automata modeling for mixed traffic with cars and motorcycles," *J. Adv. Transp.*, vol. 39, no. 3, pp. 323–349, 2005.
- [37] L. W. Lan, Y. C. Chou, Z. S. Lin, and C. C. Hsu, "Cellular automaton simulations for mixed traffic with erratic motorcycles' behaviours," *Phys. A, Stat. Mech. Appl.*, vol. 389, no. 10, pp. 2077–2089, May 2010.
- [38] B. R. Marwah and B. Singh, "Level of service classification for urban heterogeneous traffic: A case study of Kanapur metropolis," in *Proc. 4th Int. Symp. Highway Capacity*, 2000, pp. 271–286.
- [39] G. Tiwari, J. Fazio, and S. Pavitras, "Passenger car units for heterogeneous traffic using a modified density method," in *Proc. 4th Int. Symp. Highway Capacity*, 2000, pp. 246–257.
- [40] S. Putra, "The correction value of passenger-car equivalents for motorcycle and its impact to road performance in developing countries," *Procedia Social Behav. Sci.*, vol. 16, pp. 400–408, 2011.
- [41] A. Dhamaniya and S. Chandra, "Concept of stream equivalency factor for heterogeneous traffic on urban arterial roads," *J. Transp. Eng.*, vol. 139, no. 11, pp. 1117–1123, Nov. 2013.
- [42] D. Branston and H. Zuylen, "The estimation of saturation flow, effective green time and passenger car equivalents at traffic signals by multiple linear regression," *Transp. Res.*, vol. 12, no. 1, pp. 47–53, Feb. 1978.
- [43] M. Hadiuzzaman, M. M. Rahman, and M. A. Karim, "Saturation flow model at signalized intersection for non-lane based traffic," *Can. J. Transp.*, vol. 2, no. 1, pp. 77–90, 2008.
- [44] T. Nakatsuji, G. H. Nguyen, S. Tweesilp, and Y. Tanaboriboon, "Effects of motorcycle on capacity of signalized intersections," *Infrastruct. Planning Rev.*, vol. 18, no. 5, pp. 935–942, Sep. 2001.
- [45] T. Rongviriyapanich and C. Suppatrakul, "Effects of motorcycles on traffic operations on arterial streets," in *Proc. Eastern Asia Soc. Transp. Stud.*, 2005, vol. 6, pp. 137–146.

- [46] L. V. Leong, W. H. Wan Ibrahim, and A. F. Mohd, "Effect of motorcycles travel behavior on saturation flow rates at signalized intersections in Malaysia," presented at the 23rd ARRB Conf.—Research Partnering With Practitioners, Adelaide, SA, Australia, 2008. [Online]. Available: http://eprints.usm.my/13524/1/Effect_of_motorcycles_-_23rd_ARRB_Conference.pdf
- [47] C. C. Minh, K. Sano, and S. Matsumoto, "The speed, flow and headway analyses of motorcycle traffic," in *Proc. Eastern Asia Soc. Transp. Stud.*, 2005, vol. 6, pp. 1496–1508.
- [48] N. Y. Cao and K. Sano, "Estimating capacity and motorcycle equivalent units on urban roads in Hanoi, Vietnam," *J. Transp. Eng.*, vol. 138, no. 6, pp. 776–785, Jun. 2012.



Chien-Lun Lan received the B.B.A. and Ph.D. degrees from National Chiao Tung University, Hsinchu, Taiwan, in 2003 and 2008, respectively.

He is a Graduate Research Assistant with the Department of Civil and Environmental Engineering, University of Maryland, College Park, MD, USA. His research interests include traffic operation and management.



Gang-Len Chang (M'13) received the B.Eng. degree from National Cheng Kung University, Tainan, Taiwan, in 1975; the M.S. degree from National Chiao Tung University, Hsinchu, Taiwan, in 1979; and the Ph.D. degree in transportation engineering from The University of Texas at Austin, Austin, TX, USA, in 1985.

He is a Professor with the Department of Civil and Environmental Engineering, University of Maryland, College Park, MD, USA. His research interests include network traffic control, freeway traffic management and operations, real-time traffic simulation, and dynamic control of urban systems.

Dr. Chang is a member of the American Society of Civil Engineers (ASCE). He has served as the Chief Editor of *ASCE Journal of Urban Planning and Development* over the past 13 years.